

TESTING THE STANDARD MODEL

H. Gordon, W. Marciano  
Brookhaven National Laboratory, Upton, NY  
and

H.H. Williams  
University of Pennsylvania, Philadelphia, PA

K. Abe, U. Pennsylvania  
M. Chanowitz, U. California-Berkeley  
R. Cool, Rockefeller U.  
M. Derrick, ANL  
J. Friedman, MIT  
B. Gittelman, Cornell U.  
K. Gottfried, Cornell U.  
P. Grannis, SUNY-Stony Brook  
I. Hinchliffe, U. California-Berkeley  
J. Jackson, U. California-Berkeley  
H. Kagan, Ohio State U.  
P. Lepage, Cornell U.  
A. Melissinos, Rochester U.  
L. Nodulman, ANL  
T. O'Halloran, U. Illinois  
S. Olsen, Rochester U.

F. Paige, BNL  
F. Pipkin, Harvard U.  
R. Ruchti, Notre Dame U.  
M. Samuel, Oklahoma State  
K. Shinsky, U. California-Berkeley  
R. Shrock, SUNY-Stony Brook  
R. Siemann, Cornell U.  
H. Sticker, Rockefeller U.  
M. Tannenbaum, BNL  
F. Taylor, Northern Illinois U.  
M. Tuts, SUNY-Stony Brook  
H. Tye, Cornell U.  
G. Tzanakos, Columbia U.  
H. Vogel, Max Plank Institute  
D. White, BNL  
R. Wilson, Columbia U.  
J. Wiss, U. Illinois

Summary

We summarize here the results of the standard model group which has studied the ways in which different facilities may be used to test in detail what we now call the standard model, that is  $SU_c(3) \times SU(2) \times U(1)$ . Shown below are the topics considered with the names of the individuals working on each topic.

$W^\pm, Z^0$  Mass, Width

Gittelman, Gordon, Gottfried, Grannis, Jackson, Kagan, Marciano, Nodulman, Siemann, Tzanakos, Vogel.

$\sin^2 \theta_W$  and Neutral Current Couplings

Abe, Gittelman, Marciano, Pipkin, Shinsky, Taylor, White, Williams.

$W^+W^-, W\gamma$

Gordon, Nodulman, Samuel, Siemann.

Higgs

Goldberg, Grannis, Olsen, Paige, Williams.

QCD

Cool, Derrick, Friedman, Gottfried, Hinchliffe, Jackson, Lepage, O'Halloran, Sticker, Tannenbaum, Tuts, Tzanakos, Vogel, White.

Toponium and Naked Quarks

Derrick, Gittelman, Gottfried, Jackson, Olsen, Paige, Ruchti, Tye, White, Wiss.

Glueballs

Chanowitz, Tye.

Mixing Angles

Shrock.

Heavy Ions

Gottfried, Jackson, Melissinos, Wilson.

1.  $W^\pm, Z^0$  Mass, Width and  $\nu$  Counting

We first consider the production rates for  $Z^0$  and  $W^\pm$  bosons at the different facilities, that is pp,  $\bar{p}p$  and  $e^+e^-$ . Shown in Table 1 are the rates expected for luminosities integrated over approximately  $10^7$  seconds.<sup>1-5</sup>

We show the rates expected (assuming a detection efficiency of 1) for the  $Z^0$  and  $W^\pm$  decaying both leptonically and to all decay modes. The fact that there are no entries under pp and  $\bar{p}p$  for

Table 1. Production Rates of  $Z^0$  and  $W^\pm$  Bosons at Different Facilities.

	$\sqrt{s}$ (GeV)	$\int L dt$ ( $cm^{-2}$ )	$Z^0 \rightarrow \mu^+\mu^-$ $e^+e^-$	$Z^0 \rightarrow All$	$W^\pm \rightarrow \mu^\pm \nu$ $e^\pm \nu$	$W^\pm \rightarrow All$
pp	800	$10^{40}$	$6 \times 10^5$	-	$6 \times 10^6$	-
$\bar{p}p$	2000 540	$10^{37}$ $10^{36}$	$6 \times 10^3$ $6 \times 10^1$	-	$3 \times 10^4$ $3 \times 10^2$	-
$e^+e^-$	93	$2 \times 10^{38}$	$6 \times 10^5$	$10^7$	-	-
$e^+e^-$	200	$10^{39}$			$4.8 \times 10^3$	15000

$Z^0 \rightarrow all$  is a reflection of the fact that it may not be possible to study decay modes other than the pure leptonic at these machines. In contrast,  $e^+e^-$  should be sufficiently clean so that one can study all of the decay modes in a relatively clean fashion. Nonetheless we see that one will expect to observe large numbers of  $Z^0$  and  $W^\pm$  at hadron machines. This will enable the study of some of the properties of the  $W^\pm$  and  $Z^0$  such as their mass and width as discussed below. Eventually, when  $e^+e^-$  facilities at 170 to 200 GeV are available, one will be able to study the  $W^\pm$  bosons in an isolated state. However, we note that it is unlikely that such a machine will

exist before the mid-90's so that the properties of the  $W^\pm$  will initially be investigated at hadron machines.

Of particular interest, of course, is the determination of the  $Z^0$  mass which is predicted quite accurately by the present measured values of  $\sin^2\theta_W$  to be  $M_Z=93.8\pm 2.5$  GeV.<sup>6</sup> The different techniques and systematic errors for determining the mass are shown in Table 2. In pp and  $\bar{p}p$  machines, one simply

Table 2. Technique and Estimated Systematic Errors in the Determination of the  $Z^0$  Mass.

Technique	Systematic Errors	$\Delta M_Z$
pp, $\bar{p}p$ Observe mass spectrum	(1) Detector calib. (2) Possibly background Production Mechanism	200-500 MeV
$e^+e^-$ Excitation curve	(1) Radiative effects (2) Machine energy	100 MeV

observes the mass spectrum. The dominant systematic errors in determining the mass will arise from uncertainties in the absolute knowledge of the detector calibration or possibly from background or production mechanisms if these are substantially different than anticipated. It is estimated primarily from uncertainties in the detector calibration that the error in the determination of the mass of the  $Z^0$  will be between 200 and 500 MeV.<sup>7</sup> In  $e^+e^-$ , one measures the excitation curve of the  $Z^0$  by varying the machine energy and here the accuracy of such a measurement will be limited by radiative effects and also by uncertainties in the machine energy. It is estimated that one should be able to determine the mass to an accuracy of about 100 MeV rather comfortably.<sup>3-5</sup>

The techniques for determining the mass of the charged W's are a little different since it is not possible to reconstruct the mass from the leptonic decays. In pp and  $\bar{p}p$ , one may observe the  $P_T$  distribution of the e or  $\mu$  and estimate from it the mass of the  $W^\pm$  which is predicted to be  $83.0\pm 3.0$ .<sup>6</sup> This may be rendered more accurate by comparing the  $P_T$  distribution for a lepton from the  $W^\pm$  with that for a lepton from the  $Z^0$ . In this way, it is estimated that the mass may be determined to an accuracy of .5 to 1 GeV.<sup>8</sup> Shown in Figure 1 are two data samples of  $5 \times 10^4$  events generated for a hypothetical  $W^\pm$  mass of 83 GeV and of 82 GeV. It may be seen that the statistical errors are clearly sufficient to resolve these two possibilities. There may, of course, be systematic errors if there is significant background or if the  $Z^0$  and the  $W^\pm$  are produced with substantially different transverse momentum. It is anticipated, however, that the event sample should be rather clean on the high momentum side, which is what determines the mass.

At  $e^+e^-$  machines, the most accurate determination of the  $W^\pm$  mass will be performed by production of charged  $W^\pm$  pairs near threshold for an  $e^+e^-$  energy of approximately 170 GeV.<sup>3</sup> Here the uncertainties in the mass determination will arise from uncertainties in the machine energy and from statistical errors. It should be possible in a reasonable amount of running to determine the mass to an accuracy of better than 200 MeV.

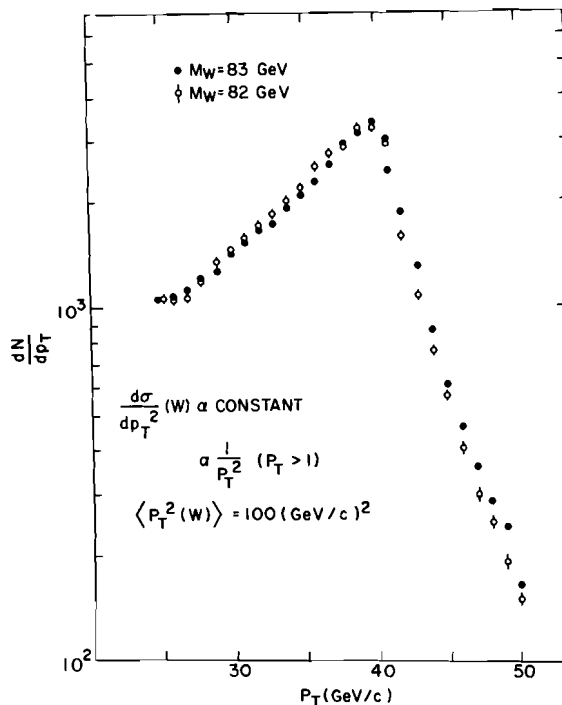


Fig. 1. Transverse momentum spectrum of leptons from the reaction  $pp \rightarrow W + \ell + \nu$  for mass of  $W=82$  and  $83$  GeV.

In electron proton machines, one will observe the effect of the  $W^\pm$  propagator as one goes to increasingly higher  $Q^2$ . The dominant uncertainties will arise from uncertainties in the knowledge of the luminosity and also in the understanding of QCD evolution at very high  $Q^2$ . One may, of course, study QCD in the neutral current, but the neutral and charged current structure functions are not identical so it is likely that there will remain some systematic uncertainty. It is estimated that one may determine the mass to approximately 5 GeV; with a significant amount of running and better understanding of the systematics it may be possible to improve this somewhat.<sup>9-12</sup> These different techniques are summarized in Table 3.

Table 3. Techniques and Systematic Errors for Determination of  $W^\pm$  Mass.

Technique	Systematic Errors	$\delta M_W$
pp, $\bar{p}p$ Observe $P_T$ spectrum. Compared to $Z^0$ .	Different $P_T$ prod. for $Z^0$ & $W^\pm$ . Possibly background.	$\approx .5$ GeV*
$e^+e^-$ (170 GeV) $W^+W^-$ excitation	Machine energy	$\approx 200$ MeV
ep Observe W propagator. Understand QCD from neutral current.	Uncertainty in luminosity & QCD effects	$\approx 5$ GeV

\*Does not include systematic effects noted. Most detector effects cancel.

It is, of course, of extreme interest to determine the  $Z^0$  width since that should tell us something about the number of neutrinos, leptons and quarks into which the  $Z^0$  can decay. Shown below

$$\begin{aligned}\Delta\Gamma_{\nu\bar{\nu}} &= 181 \text{ MeV/type} \\ \Delta\Gamma_{\ell\bar{\ell}} &= 92 \text{ MeV/type} \\ \Delta\Gamma_{u\bar{u}} &= 333 \text{ MeV/type} \\ \Delta\Gamma_{d\bar{d}} &= 425 \text{ MeV/type}\end{aligned}$$

are the partial widths for neutrinos, leptons and u and d type quarks assuming  $M_Z=93.8 \text{ GeV}$ .<sup>6</sup> These partial widths include the QCD corrections and scale like  $(M_Z^3)$ . Table 4 summarizes the different techniques for determining the  $Z^0$  width.

Table 4. Uncertainties in the Determination of the  $Z^0$  Width.

	Technique	Systematic	Uncertainties
pp, $\bar{p}\bar{p}$	Measure mass spectrum	Uncertainties in calibration stability, resolution function	100-200 MeV
$e^+e^-$	Excitation curve	Uncertainty in initial state radiation	$\approx 50 \text{ MeV}$

Again, in pp or  $\bar{p}\bar{p}$  machines, one simply measures the mass spectrum. An accurate determination of the  $Z^0$  width requires unfolding the width due to the resolution function and also requires very accurate knowledge of the absolute calibration of the detector. Small uncertainties in the absolute calibration could yield substantial effects in the measured width. It is estimated that one should be able to obtain an accuracy of approximately 100 to 200 MeV.

In  $e^+e^-$ , determination of the width is significantly more straightforward since one again studies the excitation curve and the knowledge of the machine energy is quite accurate and presumably stable. Here it is estimated that the uncertainty in knowledge of the initial state radiation, which in total contributes about 17 percent to the measured width, will limit the accuracy of the  $Z^0$  width determination to approximately 50 MeV.<sup>13</sup> It is, of course, possible if our knowledge of the radiative effects becomes more accurate that a still better precision could be obtained.

Proposal P714 at Fermilab, otherwise known as LAPDOG,<sup>7,14</sup> has studied Monte Carlo ensembles of events for different experiments with detectors of various mass resolution  $\sigma_m$ . They found that the statistical uncertainty in the observed width  $\delta\Gamma$  for each of these hypothetical experiments is related to the width  $\Gamma_{\text{tot}}$  by

$$\delta\Gamma = \left(\frac{2}{N}\right)^{1/2} \sqrt{\Gamma_{\text{tot}}^2 + (2.35\sigma_m)^2} \quad (1)$$

where N is the detected number of events.

Table 5 summarizes their estimates of the statistical error obtained for the integrated luminosities shown. They consider two different types of detectors, a high resolution detector, for example using lead glass, and an average resolution detector

Table 5. Statistical Uncertainty in the Measured Width for Different Facilities.

	$\sqrt{s}$ (GeV)	$\int Ldt$ ( $\text{cm}^{-2}$ )	$\sigma_m(\text{GeV})$	$\delta\Gamma(\text{stat.})$
pp	800	$10^{40}$	.75 (Pb Glass) 2.25 (Pb Scint)	9 MeV 16 MeV
$\bar{p}\bar{p}$	2000	$10^{37}$	.75 (Pb Glass) 2.25 (Pb Glass)	90 MeV 157 MeV
$e^+e^-$	93	$10^{38}$	.13	2 MeV

which might consist of lead scintillator shower counters. The primary point to be gained from this is that at least at high luminosity pp or  $\bar{p}\bar{p}$  and at  $e^+e^-$ , the statistical errors will be small. It is, of course, advantageous to have a detector of high resolution. It is apparent that in most cases the statistical error will be negligible compared to the systematic errors shown above.

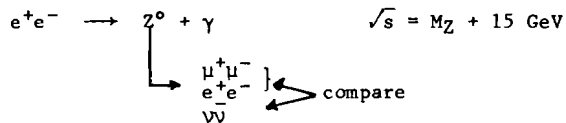
Next we concentrate on determinations of the number of neutrinos. The uncertainties in the determination of the  $Z^0$  width mentioned above lead to corresponding uncertainties in the number of neutrinos as shown below.

$$\Delta\Gamma = 181 \text{ MeV/neutrino type}$$

$$\text{pp, } \bar{p}\bar{p} \quad \delta\Gamma_Z = 100-200 \text{ MeV} + \pm (1/2 - 1) \nu's$$

$$e^+e^- \quad \delta\Gamma_Z = 50 \text{ MeV} + \pm 1/3 \nu's$$

It has been pointed out by a number of people,<sup>6</sup> however, that there may be some uncertainties in the interpretation of the width measurements, particularly if the mass of the top quark is close to one half the mass of the  $Z^0$ . It is, of course, possible in this event that the t will be observed and the corrections to the  $Z^0$  width may be made. Nonetheless, there is a cleaner experiment which promises to give the best measurement of the number of neutrinos. This experiment entails running the  $e^+e^-$  machine at an energy approximately 15 GeV above the mass of the  $Z^0$  and searching for the reaction  $e^+e^- \rightarrow Z^0 + \gamma$  where the  $Z^0$  subsequently decays into  $e^+e^-$ ,  $\mu^+\mu^-$  or  $\nu\bar{\nu}$ .<sup>15</sup>



Require  $\theta_\gamma > 20^\circ$ ,  $E_\gamma \approx 15 \text{ GeV}$  and no particles from  $6^\circ-174^\circ \rightarrow$  Very little Background.

$$\int Ldt = 6 \times 10^{37} + \pm 3\nu \quad (\text{For } N_\nu=3)$$

If one requires that the angle of the photon is larger than  $20^\circ$  and given that the energy of the photon is approximately 15 GeV, it is estimated that there should be very little background. It is estimated that one should be able to attain an accuracy as small as .1 neutrinos if one dedicates sufficient running time.

## 2. $\sin^2\theta_W$ and Neutral Current Coupling

We now go on to discuss the accuracy with which one will be able to determine  $\sin^2\theta_W$  and the neutral current coupling constants. Shown below are our

current knowledge of  $\sin^2\theta_W$ ,  $\rho$  and the approximate knowledge of the hadronic and leptonic currents.<sup>16</sup>

Current Knowledge (low  $q^2$ )

- |     |   |                           |
|-----|---|---------------------------|
| (1) | $\sin^2\theta_W (M_W) = 0.215 \pm .010 \pm .004$                      | } assumes $\rho^2 = .983$ |
|     | $\uparrow$ Statistical uncertainty $\uparrow$ Theoretical uncertainty |                           |
| (2) | $\rho = 1.010 \pm 0.020$<br>$\sin^2\theta_W (M_W) = 0.236 \pm 0.030$  | } two parameter fit       |
| (3) | Hadronic Current $\pm 2 - 3\%$  |                           |
| (4) | Leptonic Current $\pm 5 - 10\%$                                       |                           |

One of the studies made was to estimate what one could learn from more accurate measurements of the pure leptonic current using neutrino interactions,<sup>17</sup> in particular,  $\nu_{\mu}e$ ,  $\nu_{\mu}\bar{e}$ ,  $\nu_e e$  and  $\nu_e \bar{e}$  scattering. Measurement of  $\nu_e e + \nu_e \bar{e}$  should determine the sign of the interference between the charged current and the neutral current. Measurement of the reactions  $\nu_{\mu}e + \nu_{\mu}\bar{e}$  and  $\nu_{\mu}e + \nu_{\mu}\bar{e}$  with 10 percent accuracy should imply a determination of the leptonic current to an accuracy of better than 5 percent. In addition, if one measures accurately the ratio  $R = (\bar{\nu}_{\mu}e + \nu_{\mu}\bar{e})/(\nu_{\mu}e + \nu_{\mu}\bar{e})$ , one achieves a reasonably accurate determination of  $\sin^2\theta_W$ . This arises because the ratio R is very sensitive to  $\sin^2\theta_W$ .

$$\frac{\delta R}{R} \approx 9 \delta \sin^2\theta_W + \delta \sin^2\theta_W = \pm .015$$

(pure leptonic)

Substantially more accurate determinations of  $\sin^2\theta_W$  will arise, however, from the future colliders. We show in Table 6 the estimated uncertainty in  $\sin^2\theta_W$  and  $\rho$  corresponding to the accuracies in the mass determinations of the  $Z^0$  and  $W^\pm$  meson presented above.

Table 6. Uncertainties in  $\sin^2\theta_W$  and  $\rho$  from Measurement of  $M_Z$  and  $M_W$ .

pp, $\bar{p}\bar{p}$	$\delta M_Z = 200-500 \text{ MeV} + \delta \sin^2\theta_W = .0012-.003$ $\delta M_W = .5 \text{ GeV} + \delta \rho = .01$
$e^+e^-$	$\delta M_Z = 100 \text{ MeV} + \delta \sin^2\theta_W = .0006$
$e^+e^-$ (LEP II)	$\delta M_W = 200 \text{ MeV} + \delta \rho = .004$

It is seen that observations at the pp and  $\bar{p}\bar{p}$  machines will lead to quite precise determinations of these parameters while the errors corresponding to the measurements at  $e^+e^-$  are delightfully small. Recall that  $\rho = 1$  for a model in which there are any number of scalar Higgs doublets, while models with more complicated Higgs sectors, for example with triplets, in general predict  $\rho$  not equal to one.

Measurements of  $e^+e^- \rightarrow \mu^+\mu^-$  and for that matter  $e^+e^- \rightarrow \tau^+\tau^-$  or  $q\bar{q}$  near the  $Z^0$  allow determinations of  $\sin^2\theta_W$  and  $\rho$  or other parameterizations of the coupling constants, in an independent way, particularly if one is able to polarize the incident electron. We concentrate here on measurements of the reaction  $e^+e^- \rightarrow \mu^+\mu^-$ . The others have been studied in some detail in the SLC workshop.<sup>5</sup> We define the vector and axial vector, electron and muon couplings in the standard way (see below). There are then two different asymmetries of interest which can be measured. One is the so-called charged asymmetry

( $A_{CH}$ ) or forward-backward asymmetry ( $A_{FB}$ ) which is currently being measured at PEP and PETRA. This may, of course, be measured either with or without polarized electrons. However the longitudinal asymmetry  $A_L$  which is possible with polarized electrons and is even more powerful is simply to observe the differential cross section at a given angle for electrons polarized with positive helicity or negative helicity. These different asymmetries measure different combinations of the leptonic couplings  $V_e/A_e$  and  $V_\mu/A_\mu$ , as shown below.

Define  $V_e = (g_{Re} + g_{Le})/2$  electron couplings  
 $A_e = (g_{Re} - g_{Le})/2$

$A_{CH} = A_{FB} = \frac{d\sigma(A) - d\sigma(\pi-A)}{d\sigma(A) + d\sigma(\pi-A)} \Big|_{\mu^-}$  measure with polarized electron or without

$A_L(A) = \frac{d\sigma(A, P_e=+) - d\sigma(A, P_e=-)}{d\sigma(A, P_e=+) + d\sigma(A, P_e=-)}$  variation in cross section with spin flip

$A_{CH}$  (unpolarized e) measures  $\approx \left(\frac{V_e}{A_e}\right)\left(\frac{V_\mu}{A_\mu}\right)$

$A_{CH}$  (polarized) measures  $\approx V_\mu/A_\mu$

$A_L$  (polarized e,) measures  $\approx V_e/A_e$   
integral over  $\pi/2 - \alpha < \theta < \pi/2 + \alpha$

$A_L$  (polarized e,) measures  $\approx (V_e/A_e + 3/4 V_\mu/A_\mu)$   
integral over  $0 < \theta < \pi/2$

We make the assumption that the vector coupling is much smaller than the axial vector coupling as is expected in the standard model ( $V/A = 4\sin^2\theta_W - 1 = -0.14$ ) and known to be true at least for the electron coupling. The exact expressions are in the SLC Workshop proceedings. From a sample of  $10^6 Z^0$ s which should be achieved in the first year of SLC running and in a considerably shorter period of time at LEP, one obtains the statistical errors on  $\sin^2\theta_W$  and the vector, axial-vector ratios shown below:

From  $A_{CH}$  Measurements

$\delta \sin^2\theta_W \approx .003$	$\delta \sin^2\theta_W \approx .002$
$\delta (V_\mu/A_\mu) \approx .024$	$\delta (V_\mu/A_\mu) \approx .008$
no electron polarization	equal running with $P_e = +.5$ and $-.5$

From  $A_L$  Measurements

$\delta \sin^2\theta_W \approx .0009$   
 $\delta V_\mu/A_\mu \approx .008$

The effect of systematic errors depends on the particular reaction considered. For the forward-backward asymmetry measurements without electron polarization one has to ensure that the detector has identical efficiencies for  $\mu^+$  and  $\mu^-$ . This could be achieved either by rotating the detector, by changing the direction of the  $e^+$  and  $e^-$  or possibly by other means. Detector systematic errors should be particularly small however for measurements of the longitudinal asymmetry  $A_L$ .

Finally, we say just a few words about tests of electron-muon universality in the neutral current. Currently comparison of the electron coupling constants determined from  $\nu_{\mu}e$  and  $\nu_e e$  scattering, with measurements of the forward-backward asymmetry in  $e^+e^- \rightarrow \mu^+\mu^-$  should allow a comparison of the axial vector coupling constants to an accuracy of approxi-

mately 15 percent.<sup>16</sup> The uncertainty quoted above in the ratio  $V_{\mu}/A_{\mu}$ , for measurements of the longitudinal asymmetry at SLC (0.008), compared to the expected value of  $V_{\mu}/A_{\mu}$  (0.14), allows a sensitivity of approximately  $\pm 6$  percent. If the uncertainty in the ratio of  $V_e/A_e$  were comparable, one would then be able to test universality to about 10 percent. Of course, with additional running it is possible that errors could be reduced. Nonetheless, the point is that while the accuracy in the determination of the ratio is small, the expected value of this ratio is also small so that one does not obtain a very precise test. A much more precise test should be possible by comparing directly the rates for  $Z^0 \rightarrow e^+e^-$  and  $Z^0 \rightarrow \mu^+\mu^-$ . This comparison should be limited only by statistics and the uncertainty in the detection efficiency for electrons and for muons. An uncertainty in the absolute detection efficiency of  $\pm 10\%$  leads to a determination of  $A_e/A_{\mu}$  of  $\approx 7\%$ . However, the simultaneous measurement at pp and  $\bar{p}p$  machines of  $W^{\pm} \rightarrow e^{\pm}\nu$  and  $W^{\pm} \rightarrow \mu^{\pm}\nu$ , the rates of which are expected to be identical, should allow one to measure or to largely eliminate the systematic errors. In this way, it may well be possible to determine the ratio of  $Z^0 \rightarrow e^+e^-$  and  $Z^0 \rightarrow \mu^+\mu^-$  to a couple percent. This would correspond to an accuracy of 1 percent in the amplitudes for these two processes and hence would yield a precise test of electron-muon universality in the weak neutral current. The inherent cleanliness in  $e^+e^-$  machine may well allow measurements of similar accuracy.

### 3. Non-Abelian Gauge Theory and Trilinear Gauge Coupling

Assuming that we have now observed the W and  $Z^0$  bosons, that we have determined their masses (resulting in precise determinations of  $\rho$  and  $\sin^2\theta_W$ ), and that we have furthermore determined accurately the coupling constants, we still want to test one of the most crucial parts of the standard model, namely the gauge-gauge coupling characteristic of a non-Abelian gauge theory. We concentrate here on possibility to observe the  $Z^0 WW$  coupling. Table 7 lists the production rates for  $W^+W^-$  at pp,  $\bar{p}p$  and  $e^+e^-$  machines.<sup>18</sup>

Table 7. Production Rates for  $W^+W^-$ .

	$\sqrt{s}$ (GeV)	$\int L dt$ ( $cm^{-2}$ )	Produced Events	Useful Events ( $\mu\nu$ )( $e\nu$ )	( $l\nu$ )( $qq$ )	Signal/ Noise
pp	800	$10^{40}$	1000	9	168	Maybe OK
$\bar{p}p$	2000	$10^{37}$	70	.6	12	Maybe OK
$e^+e^-$	180	$10^{39}$	15000	135	2520	Clean

For  $e^+e^-$  one must, of course, await the advent of LEP II with center of mass energies in excess of 170 GeV. The table lists the number of events obtained in total, the number if one demands one W to decay leptonically and the other one hadronically, and the number if one demands that both W's decay leptonically. One might expect that observation of the large  $P_t$  unaccompanied lepton from one W decay together with two jets reconstructing to a mass of approximately 83 GeV would result in an identifiable sample in high luminosity pp interactions. However, this has not been clearly demonstrated at the present time. In  $e^+e^-$  one should obtain a large sample of clean events even assuming that one demands one of the W's to decay leptonically. A detection efficiency of .7 has arbitrarily been assumed in these numbers. To get an idea of whether the

observation of one or two hundred identifiable  $W^+W^-$  events in hadron-hadron interactions would allow one to make significant conclusions regarding the gauge-gauge coupling, we show in Figure 2 the total cross section for  $W^+W^-$  production as a function of  $\sqrt{s}$ .<sup>3</sup> For

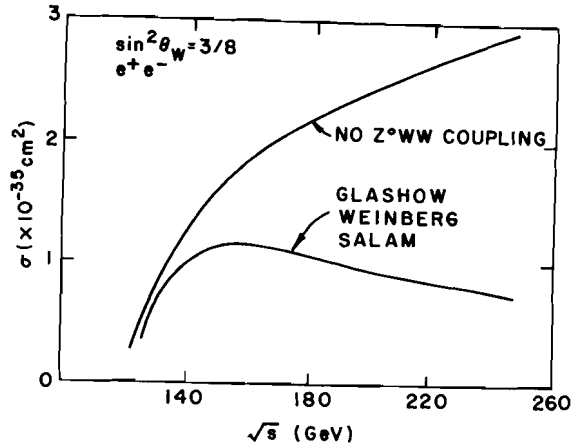
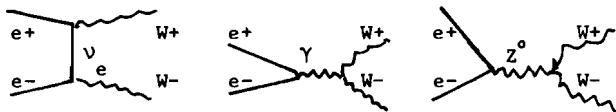


Fig. 2. Cross section for  $e^+e^- \rightarrow W^+W^-$  as a function of  $\sqrt{s}$ .

simplicity, the cross section shown is for  $e^+e^-$ . The cross section is shown for the Glashow-Weinberg-Salam model and also for the case in which one assumes that there does not exist a  $Z^0 WW$  coupling. (The latter, of course, would violate unitarity at sufficiently high energy.) The important point is whether there exists a substantial difference for these two cases after one has correctly integrated over the structure functions of the proton. If so, then a clean sample of  $W^+W^-$  events in pp ( $\bar{p}p$ ) might allow some early conclusions regarding the existence of gauge-gauge couplings. However, it is unequivocal that the cleanest way to test for these couplings is at  $e^+e^-$  machines.

We show below the three diagrams expected in  $e^+e^-$  to contribute to  $W^+W^-$  production, the exchange diagram and the annihilation diagrams involving the photon and the  $Z^0$ .



Shown in Figure 3 is the contribution of each of these diagrams and that of the interference terms to the cross section as a function of  $\sqrt{s}$ . The idea is to use the angular distribution to untangle the interference term to allow a more accurate comparison with the theoretical expectations. Figure 4 shows an estimate performed by M. K. Gaillard,<sup>3</sup> of the accuracy that would result from 100  $W^+W^-$  pairs observed at a series of different energies. Also shown are the results expected for the Glashow-Salam-Weinberg model where  $\sin^2\theta_W = 0.25$  and for the case of no  $Z^0 WW$  coupling. It should be noted, however, that the maximum energy of LEP II may correspond more closely to values of  $s/s_{\text{threshold}}$  of 1.5 than to values of 3.

Another interesting reaction which can perhaps be studied in a hadron hadron machine is the search for the final state  $WY + X$ .<sup>19</sup> The diagrams which are expected to contribute are

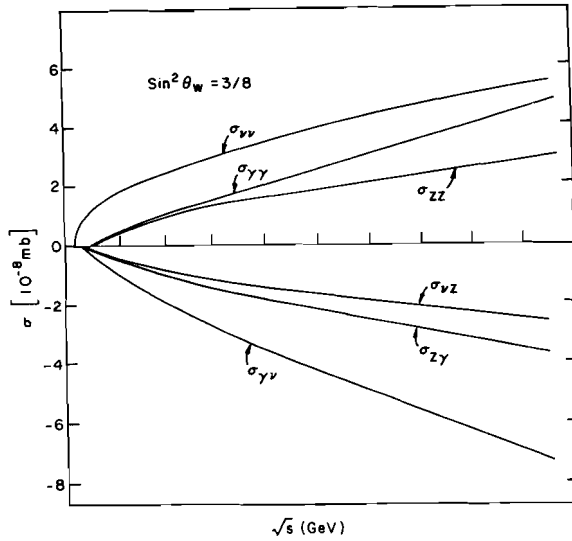
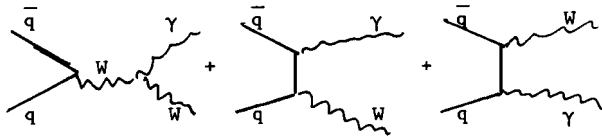


Fig. 3. Contributions to  $e^+e^- \rightarrow W^+W^-$  from the diagrams mentioned in the text as a function of  $\sqrt{s}$ . Shown below zero are the contributions due to the interference of the various diagrams.



Observation and measurement of this process would determine the magnetic moment of the W,  $\mu = e/2M_W(1+\kappa)$ . In non-Abelian gauge theories  $\kappa$  is predicted to be 1. At a center of mass energy of 800 GeV for pp interactions, the cross section for this process is anticipated to be approximately  $7 \times 10^{-36} \text{ cm}^2$ .<sup>19</sup> For  $\int L dt = 10^{40} \text{ cm}^{-2}$  and assuming that one requires the transverse momentum of the photon to be larger than 20 GeV, one expects to obtain approximately 600 events. An estimate of the background has been made by considering events in which a W is produced together with an additional jet which fragments in such a way that one obtains a largely unaccompanied  $\pi^0$  with a  $P_T$  larger than 20 GeV. One obtains from this calculation approximately 500 events.<sup>8</sup> Thus, assuming a detector with a  $\gamma/\pi^0$  separation of better than 5 to 1, it might be possible to observe this reaction cleanly. Measurements of the rate and the angular distribution are sensitive to the prediction of the magnetic moment of the W from the gauge theory. The different angular distributions expected for different values of the magnetic moment are shown in Figure 5.<sup>20</sup>

#### 4. Higgs Bosons

Assuming with our usual presumptuousness that studies of the gauge-gauge coupling yield the results which we expect, there nonetheless remains a crucial test of the standard model, that is, the discovery and study of the properties of the Higgs boson.<sup>21</sup> While the standard model can easily accommodate more than one such boson, we assume the simplest case where there exists a single, neutral, scalar boson. We discuss three different ways in which it might be observed in  $e^+e^-$  collisions and an intriguing possibility for observing very heavy Higgs bosons in pp or  $p\bar{p}$  interactions if sufficient luminosity can be attained.

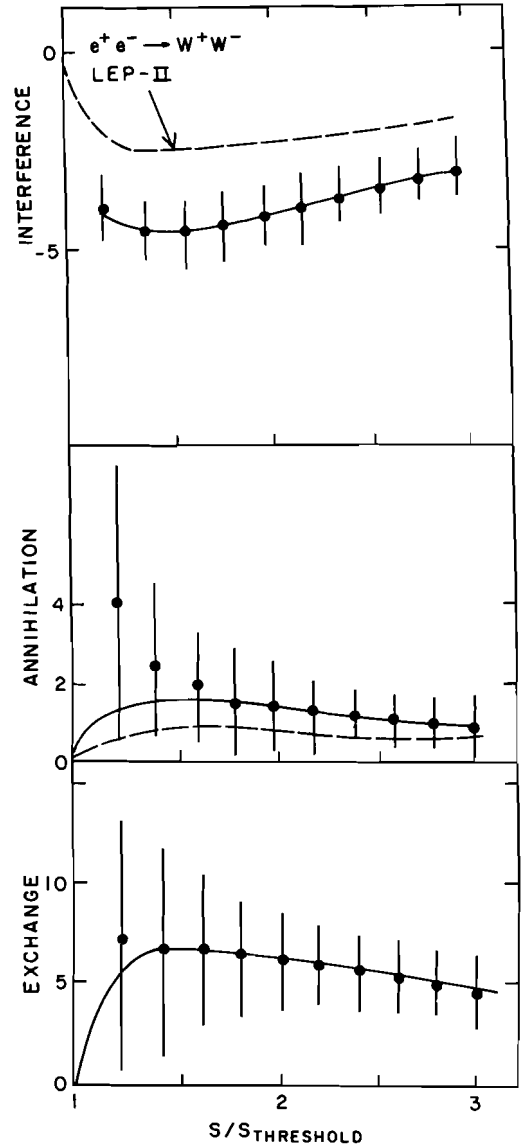


Fig. 4. Expected error from 100 events at 10 energies in determining the interference, annihilation and exchange contribution in  $e^+e^- \rightarrow W^+W^-$ . Solid curve is expected from a non-Abelian gauge theory whereas the dashed line is for no  $Z^0 WW$  coupling.

We first consider the case in which one has discovered toponium, the bound state of t and the  $\bar{t}$  quark. If one then sits on the toponium resonance  $\Theta$  with an  $e^+e^-$  machine, one expects to observe a substantial decay rate into Higgs plus a photon.<sup>4,13</sup> We arbitrarily assume the toponium has a mass of 75 GeV and if we furthermore assume an average luminosity of  $1.1 \times 10^{31} \text{ cm}^{-2} \text{ sec}^{-1}$ , with an energy spread of the beam of approximately 70 MeV, one obtains, after including radiative effects, an R value of approximately 4. This should then yield approximately 120 events a day. Assuming the theoretical expectations for the relative decay rates of toponium into Higgs plus photon versus  $\mu^+\mu^-$ , and also the expected branching ratios for toponium into  $\mu^+\mu^-$  versus the total decay rate, one anticipates a branching ratio of toponium into Higgs plus photon of 1 to 2 percent depending on the Higgs mass.

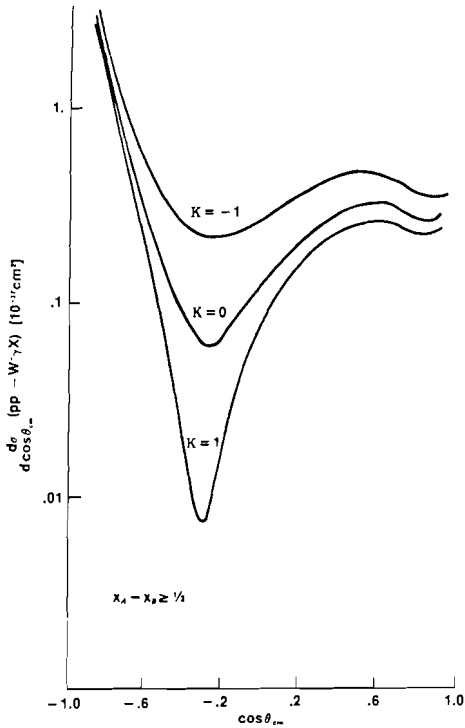


Fig. 5. Angular distribution expected in  $pp \rightarrow W\gamma + x$  where  $\cos\theta$  is the angle between the proton and the  $\gamma$  in the  $W\gamma$  rest frame.  $\kappa$  (the magnetic moment of the  $W$ ) is predicted to be +1 by the standard model.  $x(W\gamma) > 1/3$ .  $E_Y > 30$  GeV

$$\frac{\Gamma(\theta \rightarrow H^0 + \gamma)}{\Gamma(\theta \rightarrow \mu^+ \mu^-)} = \frac{G_F M_\theta^2}{2\sqrt{2}\pi\alpha} \left(1 - \frac{M_H^2}{M_\theta^2}\right) F(M_\theta) \approx 0.25$$

$$\frac{\Gamma(\theta \rightarrow \mu^+ \mu^-)}{\Gamma(\theta \rightarrow \text{all})} = 0.08$$

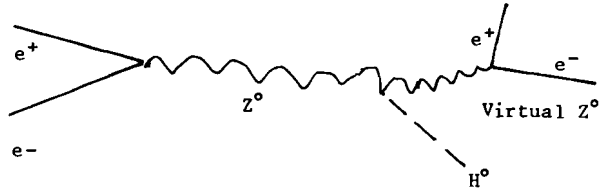
Hence, for an integrated luminosity of  $10^{38} \text{ cm}^{-2}$  one would expect to obtain 40 to 100 such events. One of the dominant background processes will presumably be the decay of toponium to a photon plus two gluons. This is expected to occur with a total decay rate only four to six times that of the decay into Higgs and, since the photon is non-monochromatic, it should provide little background to the monochromatic photon expected in the Higgs decay. It is thus anticipated that this process should be reasonably clean. The number of events expected as a function of the mass of Higgs is presented in Table 8.

Table 8. Summary of Rates for Higgs Production at  $e^+e^-$  Machines.

$$\int L dt = 10^{38} \text{ cm}^{-2}$$

Final State	$t\bar{t} \rightarrow H^0 + \gamma$	$Z^0 \rightarrow e^+ e^- H^0$	$H^0 + Z^0 \rightarrow e^+ e^-$
	$\sqrt{s} = M_{t\bar{t}}$ (75 GeV)	$\sqrt{s} = M_{Z^0}$	$\sqrt{s} = M_{Z^0} + 1.4 M_{H^0}$
$M_{H^0}$ (GeV)	Events	Events	Events
10	100	400	120
20	92	90	40
40	71	12	10
60	36	1	6

Another reaction which has been widely considered as a good one in which to search for the Higgs boson is to search for the reaction  $e^+e^- \rightarrow Z^0$ , the  $Z^0$  then decaying to a virtual  $Z$  plus the Higgs boson, with the virtual  $Z$  subsequently decaying to  $\mu^+\mu^-$  or  $e^+e^-$ .<sup>22</sup>



The expected rate for this decay relative to the decay of a  $Z$  to  $\mu^+\mu^-$  is shown in Figure 6 as a function of the ratio of the Higgs mass to the mass of the  $Z$ .<sup>4,22,23</sup> One may see that a reasonable

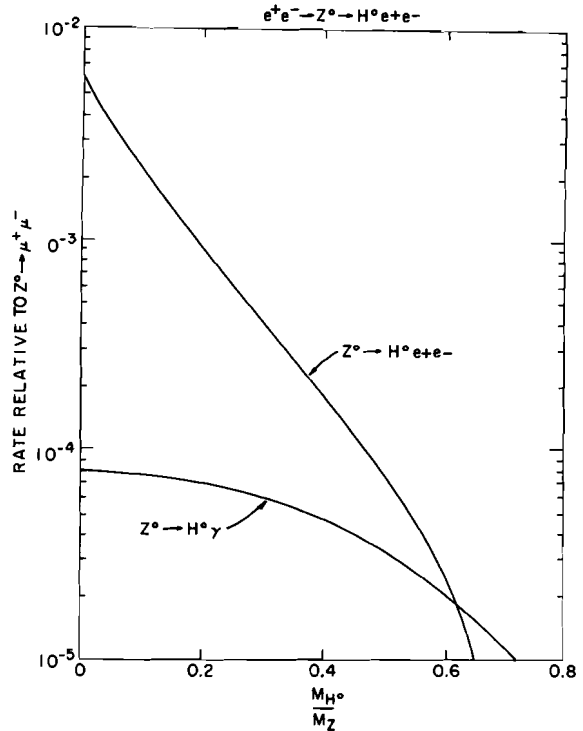


Fig. 6. Ratio of  $(Z^0 \rightarrow e^+e^- H^0)/(Z^0 \rightarrow \mu^+\mu^-)$  as a function of the ratio of the mass of  $H^0$  to mass of  $Z^0$ .

number of events may be obtained up to a Higgs mass of approximately 40 to 50 GeV. The particular signature for this process is to reconstruct the  $e^+e^-$  and determine the mass recoiling. Figure 7 presents the result of some Monte Carlo calculations indicating the separation of the signal from the background for a Higgs mass of 10 GeV.<sup>5</sup> In fact, as the Higgs mass gets heavier, the missing mass resolution should improve as the electrons will then be of lower energy. Nonetheless, for masses above 40 GeV the rate becomes quite small and the sensitivity of this technique is probably limited to masses of that order.

A third possibility for searching for the Higgs boson with an  $e^+e^-$  machine is to run with the center mass energy larger than the mass of the  $Z^0$  by approximately 1.4 times the Higgs mass.<sup>13,24</sup> In this case the  $e^+e^-$  can go to a virtual  $Z^0$  which then decays to a real  $Z$  and a real Higgs.

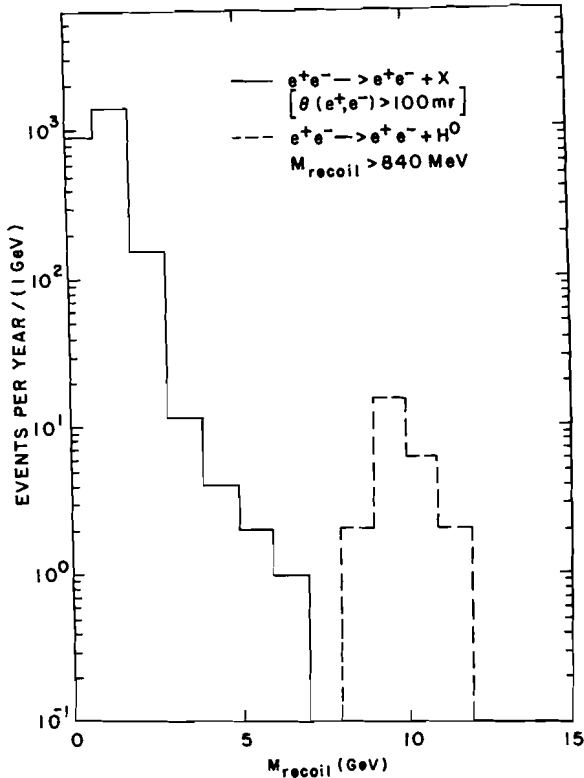
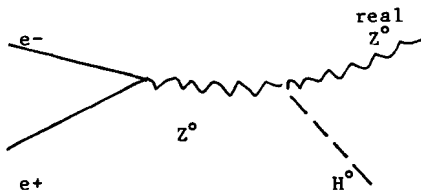


Fig. 7. Mass recoiling from  $e^+e^- \rightarrow Z^0 \rightarrow e^+e^- + X$  where the dashed line indicates the  $H^0$  production for  $M_{H^0} = 10$  GeV and the solid line is an estimate of all backgrounds.



One would reconstruct the  $e^+e^-$  effective mass which would equal that of the  $Z^0$  and determine the missing mass recoiling against the Z. Figure 8 shows the

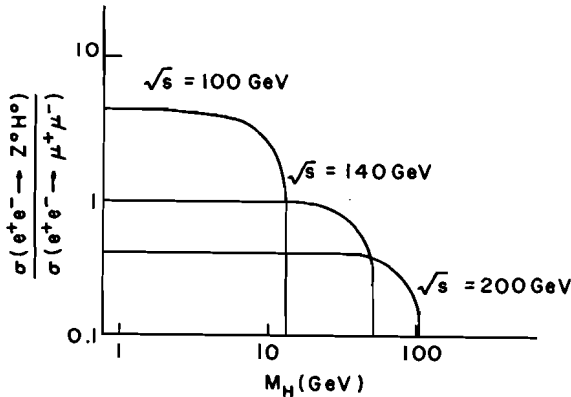
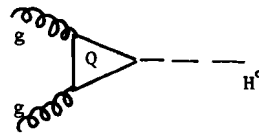


Fig. 8. Ratio of cross section for producing  $H^0$  to  $\mu^+\mu^-$  in  $e^+e^-$  interactions at various center of mass energies as a function of  $M_{H^0}$ .

expected branching ratio into  $Z^0$  plus Higgs compared to the rate for  $e^+e^- \rightarrow \mu^+\mu^-$  as a function of the Higgs mass for different values of the center of mass energy. Once the center of mass energy has been chosen, one has equal sensitivity to Higgs of any mass which is kinematically accessible. The optimum rate may be obtained by setting the center of mass energy equal to the mass of the  $Z^0$  plus 1.4 times the Higgs mass. Nonetheless, since the Higgs mass will undoubtedly not be known, one has little choice other than to run at the maximum center of mass energy which is accessible. One of the backgrounds considered,  $e^+e^- \rightarrow t\bar{t}$  which then can decay to  $e^+e^- + X$ , is comparable in magnitude to the signal before any cuts are made. It is therefore anticipated that after suitable cuts this reaction should yield little background and a clean signal for the Higgs meson should be obtained if it exists in the accessible mass range. Table 8 summarizes the rates available for the three different techniques of searching for the Higgs in  $e^+e^-$  collision as a function of the Higgs mass. It should be noted that the numbers presented for the technique of running at a center of mass energy above the  $Z^0$  have assumed in each case that one picked the center of mass energy yielding the optimum rate for that particular value of the Higgs mass. Hence these numbers are undoubtedly somewhat of an overestimate. It may also be observed that the technique of exciting the toponium resonance yields the best rate for heavy Higgs. Recall, however, that it was assumed that the mass of toponium was 75 GeV. If the mass of toponium is in fact significantly lighter, then clearly one is limited to a lower mass range.

We now go on to consider an interesting possibility for the production of very heavy Higgs with pp and  $\bar{p}p$  machines.<sup>25</sup> The dominant diagram for Higgs production in these machines is expected to be by the process of gluon fusion.



The cross section for this process was first calculated by Georgi et al.,<sup>26</sup> and they obtained

$$\frac{d\sigma_H}{dy} = \frac{\pi}{32} \left( \frac{\alpha_s(M_H^2)}{\pi} \right)^2 \frac{G_F}{\sqrt{2}} \frac{N^2}{9} \tau F_G(\sqrt{\tau} e^{+y}) F_G(\sqrt{\tau} e^{-y})$$

$$F_G(x) = \text{gluon structure function}$$

$$\tau = \frac{M_H^2}{s}$$

$$N = \sum_Q I_Q \quad I_Q = 3 \int_0^1 dx \int_0^{1-x} dy \frac{1-4xy}{1-xy} \frac{M_H^2}{M_Q^2}$$

$N$  is sensitive to the value of  $M_t$  and the possible existence of heavier fermions.

Taking  $N=1$ , the cross section for producing a Higgs of mass 200 GeV is computed in a separate contribution to these proceedings.<sup>25</sup> At  $\sqrt{s}=800; 2,000;$  and 10,000 GeV; the cross sections are 0.8, 15 and  $380 \times 10^{-38} \text{ cm}^2$ .

A point of considerable interest is that for a Higgs boson mass larger than twice the mass of the  $W$  or twice the mass of the  $Z^0$ , the decays of the Higgs will be entirely dominated by  $H^0 \rightarrow W^+W^-$ ,  $H^0 \rightarrow Z^0Z^0$ . The branching fraction may be readily evaluated from



$$\Gamma_{VV} = \frac{G_F M_V^2}{8\pi/2} M_H \frac{(1-x)^{1/2}}{x} (3x^2 - 4x + 4) \left(\frac{1}{2}\right)$$

↑  
for  $Z^0$

$$x = \left(\frac{2m_V}{M_H}\right)^2$$

and is plotted in Figure 9. The ratio of the  $Z^0 Z^0$  branching ratio to that of  $W^+ W^-$  rapidly approaches 1/2 once the Higgs mass is above the  $Z^0 Z^0$  threshold. For the particular case  $M_H = 200$  GeV,  $\sqrt{s} = 10,000$  GeV and  $\int L dt = 10^{40} \text{ cm}^{-2}$ , one would expect to have approximately 7,300  $H^0 \rightarrow Z^0 Z^0$  and 23,000  $H^0 \rightarrow W^+ W^-$ .<sup>25</sup> Assuming that we demand that at least one of the  $W$ 's or  $Z^0$ 's decays leptonically, we would then have the following number of events of different types<sup>25</sup>

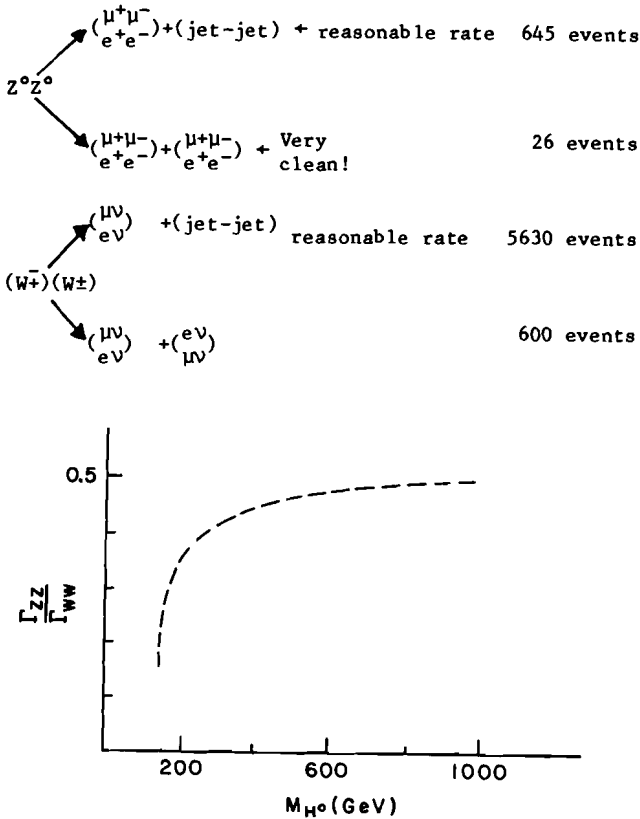


Fig. 9. Ratio of  $H^0 \rightarrow Z^0 Z^0$  to  $H^0 \rightarrow W^+ W^-$  as a function of the mass of the  $H^0$ .

Clearly the category where both  $Z^0$ 's decay to  $e^+ e^-$  or  $\mu^+ \mu^-$  is extremely clean and well identified. The only background to this sample of events is presumably from other processes producing  $Z^0 Z^0$ . One might also hope that having demanded that one of the bosons decay leptonically, the resulting sample would be sufficiently clean that one would be able to reconstruct the effective mass of the two jets to see if they in fact came from a  $W$  or a  $Z$  boson. A study of the backgrounds are given elsewhere on these proceedings.<sup>25</sup> The conclusion reached is that a statistically significant signal would be seen above background at  $\sqrt{s} = 10,000$  GeV at  $\int L dt = 10^{40} \text{ cm}^{-2} \text{ sec}^{-1}$ . At lower energies, a detectable signal would require a larger Higgs production cross section than we have assumed. This may occur if  $|N| > 1$  which would be the case if new heavy quarks exist and contribute to the gluon fusion amplitude. While a really careful study of the background has not been undertaken, we have

considered a few possibilities which leave room for optimism at the present time.<sup>25</sup>

### 5. QCD (Dynamics)

We now go on to study the other part of our standard model, namely, quantum chromodynamics (QCD). We make a somewhat artificial distinction in our discussion by considering first what one might call dynamics, that is, reactions in which we try to identify or see evidence of particular scattering processes involving gluons and quarks. We then go on to consider various techniques for trying to determine  $\alpha_s(Q^2)$ . Clearly the distinction between these two is somewhat artificial.

We first consider tests in  $e^+ e^-$  and  $ep$  interactions, searching for gluon radiation, that is, for three jet events and four jet events. Figure 10 shows different diagrams contributing to the production of two, three and four jet type events. While

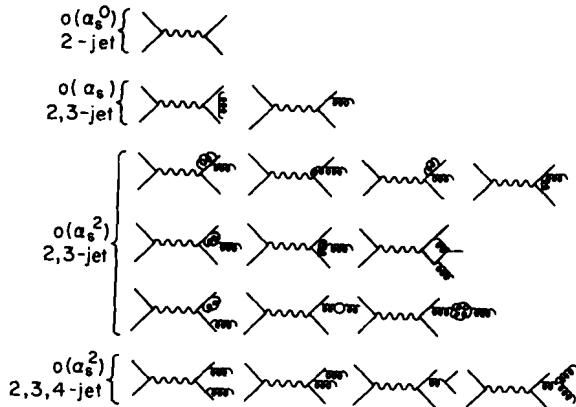


Fig. 10. Various diagrams that contribute to  $e^+ e^- \rightarrow 2, 3,$  and  $4$  jets. The diagrams are arranged by the order of  $\alpha_s$ .

there are a relatively large number of diagrams, the situation is relatively clean since the gluons couple only to the outgoing quarks. The mean transverse momentum squared of the outgoing hadrons is believed to arise from two contributions, the non-perturbative part due to the fragmentation process plus the transverse momentum expected in QCD due to gluon radiation. The importance of the non-perturbative piece is expected to decrease approximately as  $1/s$ . An estimate of the relative contributions of QCD and the fragmentation is obtained from Figure 11 which shows measurement of the energy correlation for the CELLO experiment at PETRA.<sup>27</sup> It may be seen that the contribution from fragmentation is large and hence it is not surprising that it complicates the understanding of the QCD effects at present  $e^+ e^-$  energies.

The size of the fragmentation effects relative to those of QCD are expected to be substantially smaller at higher  $e^+ e^-$  energies such as at the  $Z^0$  factories. However, if the  $t$  quark mass is large but still less than half the  $Z^0$  mass, those decays may complicate the separation of 2 jet, 3 jet and 4 jet event types. If the  $t$  is indeed heavy, one would like to run with an  $e^+ e^-$  center of mass energy just below  $t\bar{t}$  threshold.

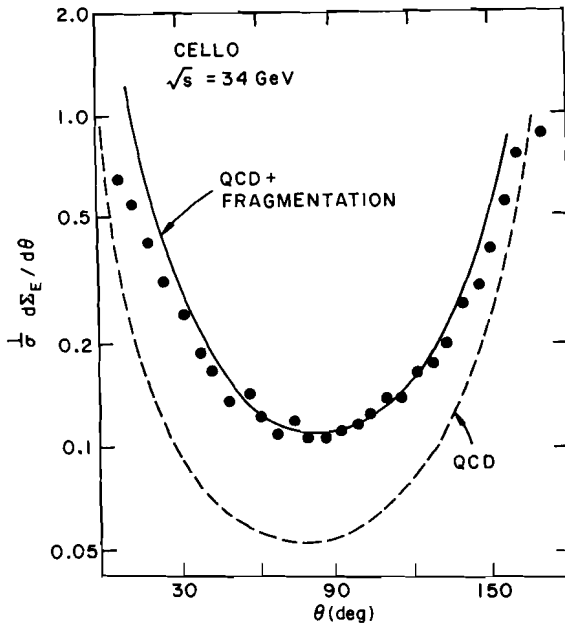


Fig. 11. The weighted energy-energy correlations. Solid line shows the effect of adding the parton fragmentation to the pure QCD prediction (dashed line).

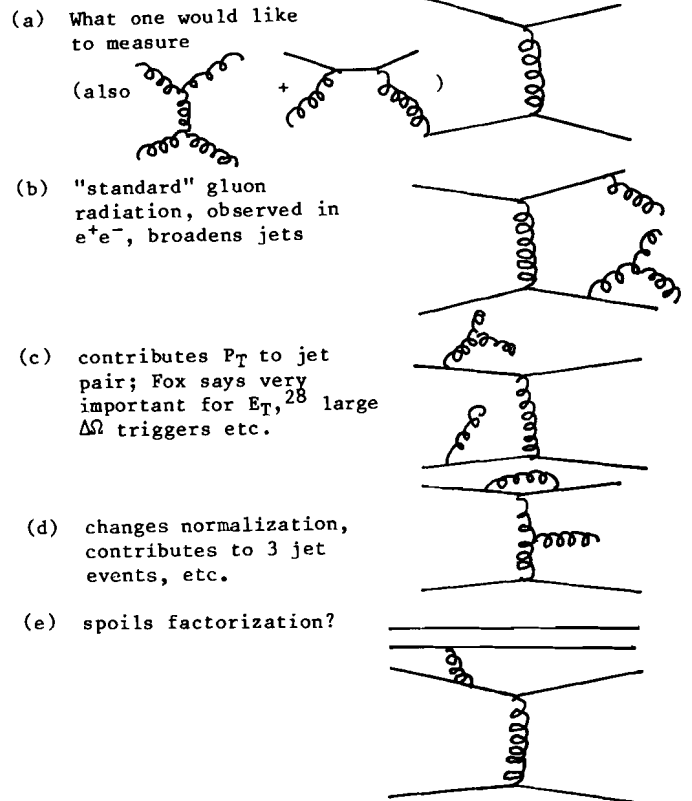
The study of gluon radiation in ep scattering has certain advantages. In particular, by measuring the momentum and angle of the outgoing electron one can predict the direction of the hadron jet. In addition, the scattering will take place primarily from u and d type quarks. A disadvantage is that in this process one may have gluons coupling to the incident and the outgoing quarks. This may complicate the theoretical predictions. Table 9 presents a comparison of event rates and the  $Q^2$  available for jet production in  $e^+e^-$  and ep facilities. It should also be

Table 9. Comparison of Rates and  $Q^2$  For Jet Production in  $e^+e^-$  and ep.

	ep (10 x 1000)	$e^+e^-$ (20 x 20)	$e^+e^- (Z^0)$
$\int Ldt$	$4 \times 10^{38}$	$4 \times 10^{38}$	$4 \times 10^{38}$
EVENTS ( $Q^2 > 1000 \text{ GeV}^2$ )	100,000	100,000	$10^7$
1 Gluon Event	10,000	$\sim 15,000$	$\sim 2 \times 10^6$
2 Gluon Events	$\sim 1,000$	$\sim 1,000$	$\sim 3 \times 10^5$
$Q^2$	$> 1,000$	400	2,500

noted that it is important to analyze events at different center of mass energies to better understand the effect of fragmentation functions, and that gluon jets, if they can be isolated, should show a faster growth in the mean transverse momentum relative to the jet axis because of the triple gluon coupling.

Next, we go on to the study of quantum chromodynamics in hadron-hadron interactions. A number of the different types of diagrams, by no means complete, are shown below.



Diagrams of type "a" are the simplest scattering processes which one would like to measure quantitatively. Those of type "b" include gluon radiation from the outgoing quarks analogous to that observed in  $e^+e^-$  interactions. Complicating the understanding of these two types of diagrams, however, are contributions from Feynman graphs of type "c" through "e". Currently our knowledge is not sufficiently good to determine whether these additional diagrams will hopelessly complicate our understanding of the basic processes or whether, at least in some kinematical regions, the contributions from these higher order diagrams may be manageable. It has recently been observed in experiments at the SPS and Fermilab fixed target program that triggers requiring a large transverse energy in a large solid angle are dominated by events with large multiplicity and cylindrically symmetric configurations; that is, no clear evidence for jet-like events was observed. It may be anticipated, however, that, since the observed cross sections fall off exponentially as a function of  $E_T$ , at some sufficiently large value of transverse momentum hard scattering processes may begin to dominate the cross section. Indeed, such a behavior has now been observed by the UA2 collaboration at the pp collider at the SPS and by the AFS collaboration at the ISR.<sup>29</sup> Their results are shown in Figure 12.

Another important point is that the size of the jets should remain well collimated even as one goes to increasingly higher energies. Figure 13 shows the distribution of  $l-T$  where  $T$  is the thrust, observed by the Pluto collaboration at PETRA, together with the expectations from quantum chromodynamics. Table 10 presents information related to the size of the jets obtained from a typical Monte Carlo program (ISAJET) which has been tuned to fit the data from PEP and PETRA.<sup>32</sup> It presents the fraction of the jets for which greater than 70% of the energy is contained within a cone of half angle,

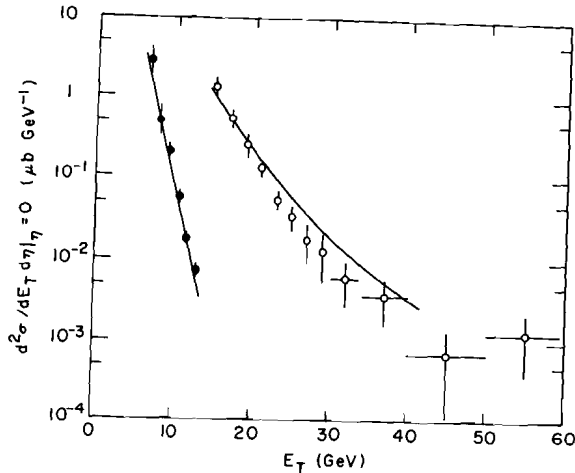


Fig. 12. Inclusive single jet cross section vs.  $E_T$  for pp collisions at  $\sqrt{s}=63$  GeV (closed circles) and pp collisions at  $\sqrt{s}=540$  GeV (open circles).<sup>29</sup> Solid line is the prediction from ISAJET<sup>30</sup> using the Baier et al.<sup>31</sup> structure functions.

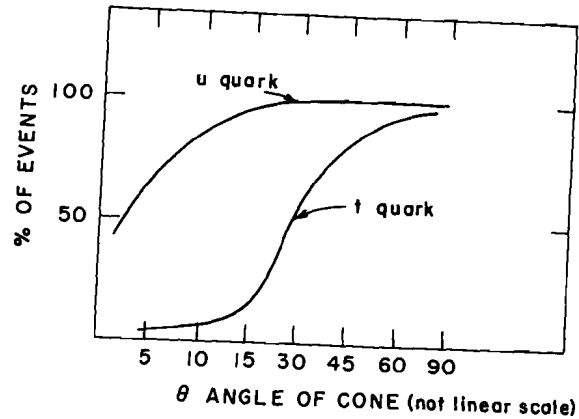


Fig. 14. Fraction of events with more than 70% of the energy within a cone of angle  $\theta$  vs.  $\theta$  for u quarks and t quarks with mass 80 GeV.

should also be noted that observations of high  $P_T$  jets by the UA2 collaboration verify that these jets behave approximately as expected even with very large transverse momentum. Thus it is to be anticipated that hard scattering processes, even if at very large transverse momentum, can be well identified. To give an indication of the rate, Figure 15 presents the

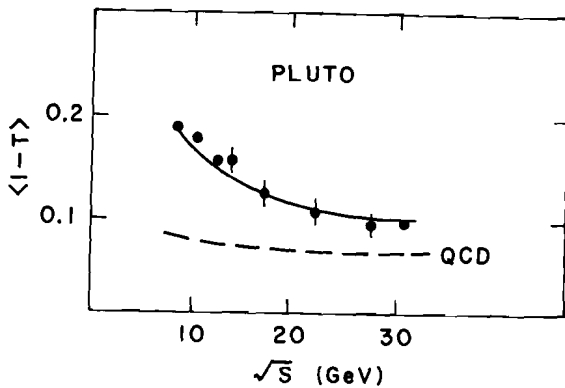


Fig. 13.  $\langle |1-T| \rangle$  vs. center of mass energy. Dashed line is expected from pure QCD while solid line includes the fragmentation functions.

Table 10. Measures of the Size of Jets vs. Momentum.

Range of $P_T$ (GeV)	Quark Type	% of Jets with >70% of Energy in 30° Cone	$\langle \text{Sphericity} \rangle$
50-100	u	$\sim 100\%$	.11
	t (20 GeV)	$\sim 97\%$	.12
150-200	u	$\sim 100\%$	.10

↑  
no growth  
in sphericity

$\theta$ , equal to  $30^\circ$ . It also presents the mean sphericity expected for jets ranging in transverse momentum from 50 to 200 GeV. The mean sphericity, and hence the mean opening angle, is expected to be approximately constant. More detailed information concerning the fraction of energy contained as a function of the angle  $\theta$  of the cone is shown in Figure 14. It

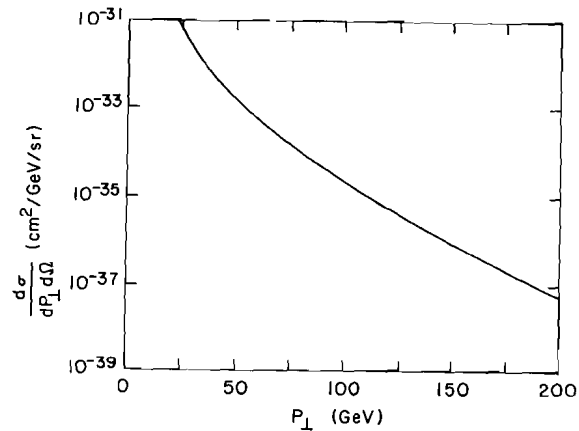


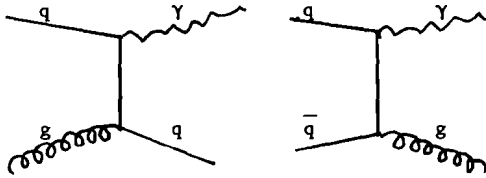
Fig. 15. Inclusive single jet cross section vs.  $P_T$  for pp collisions at  $\sqrt{s}=800$  GeV predicted by ISAJET.<sup>30</sup>

expected cross sections as a function of transverse momentum for events up to several hundred GeV. For a high luminosity pp or pp machine capable of attaining an integrated luminosity of approximately  $10^{40}$   $\text{cm}^{-2}$ , one obtains as many as 10,000 events per GeV for transverse momenta in the vicinity of 200 GeV/c. Thus, while the interpretation of hard scattering processes in hadron-hadron interactions is not as clean as in  $e^+e^-$ , it is anticipated that one can measure such processes up to very large  $Q^2$ ; for example, up to 200,000  $\text{GeV}^2$  for machines currently under construction, such as TEV I or ISA. At a minimum, it may be anticipated that such studies will be very important in the search for new interactions, quark substructure or gross breakdowns of QCD. In particular, we note that it has been pointed out by E. Eichten at

this study that any quark substructure would lead to a contact term which would behave as a point interaction. This additional contribution would lead to a very significant flattening of the cross section as a function of  $P_T$ .

Study of high mass lepton pair production, in particular the  $P_T$  and  $x$  dependence of the lepton pairs, and the characteristics of associated hadrons, has been and continues to be a topic of considerable interest. Two of the outstanding problems are (1) to understand the disagreement (by a factor of  $K \approx 2$ ) between the calculated and observed cross sections and (2) to compare the observed  $P_T$  dependence with that calculated according to QCD. The availability of measurements of the lepton pair continuum, and of  $Z^0$  production, over a wide range of  $P_T$ ,  $x$ , and  $\sqrt{s}$  would provide important tests of our current understanding.

Another process of considerable interest is high transverse momentum single photon production which can proceed by the diagrams shown below.



It will, however, be important to have high luminosity in order to reach the large values of  $x_T$  at which these processes dominate. This particular reaction has been suggested as an excellent way to isolate gluon jets in pp collisions and hence to study gluon fragmentation.

Other tests which will no doubt also be important are comparisons of large  $E_T$  events, single particle production, and energy correlations as a function of angle with the predictions of QCD. Many details of such tests are given in the contribution to these proceedings by M. J. Tannenbaum.<sup>33</sup>

#### 6. QCD (Measurements of $\alpha_s$ )

We now go on to the second half of our somewhat artificial division of tests of QCD: methods of measuring  $\alpha_s$ .<sup>34</sup> Figure 16 shows schematically the expected behavior of  $\alpha_s$  as a function of  $Q^2$ , together with an indication of the various values of  $Q^2$  that are probed by particular experiments and accelerator facilities. One would like certainly to obtain a measurement of  $\alpha_s$  accurate to approximately 10%, and we take this as a guide in our discussions of various experiments. Table 11 presents a brief summary of some of the different techniques, with comments as to the reliability of the theoretical predictions and the possibilities for the experimental measurements. It should be noted that currently no test is considered to be satisfactory in both the theoretical and the experimental domain though it is generally concluded that the value of  $\Lambda_{\overline{MS}}$  is likely to be in the vicinity of .2 GeV. We now go on to discuss a few of these measurements in more detail.

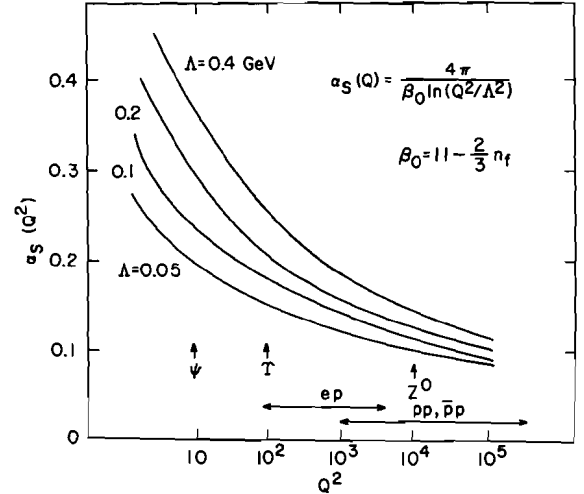


Fig. 16.  $\alpha_s(Q^2)$  vs.  $Q^2$  for various values of  $\Lambda_{\overline{MS}}$ .

Table 11. Precision Tests of QCD: Determination of  $\alpha_s$  or  $\Lambda_{\overline{MS}}$ . Theoretical reliability ranges from excellent (✓✓) to fair (✓). Topics where there exists some quantitative comparison of theory and experiment and an attempt to determine  $\alpha_s$  are indicated by a ✓ under the column T-E.

Process	Theory	Exp	T-E
R in $e^+e^-$	✓✓	Needs 1% accuracy?	
$e^+e^- \rightarrow$ jets	✓✓	At PEP & PETRA energies, effects of fragmentation are large.	✓
$Z^0 \rightarrow$ jets	✓✓	Fragmentation effects smaller; background from t quark.	
$ep$ ted, $\nu p$	✓✓	Requires 2% accuracy for $F_2^{ep}$ & $F_2^{ep}$ .	✓
$\frac{\Gamma(\eta_b \rightarrow gg)}{\Gamma(\eta_b \rightarrow \gamma\gamma)}$	✓✓	Difficult	
$B_{\mu\mu}(T)$	?	Easy	✓
$\frac{\Gamma(T \rightarrow \gamma gg)}{\Gamma(T \rightarrow 3g)}$	✓✓	$\pi^0$ Background?	
Hyperfine splitting ( $T-\eta_b$ ; $\Psi-\eta_c$ )	?	Looks good	✓

One of the most reliable theoretical calculations, and hence one of the results most eagerly sought, is the value of the ratio of  $e^+e^- \rightarrow$  hadrons to  $e^+e^- \rightarrow \mu^+\mu^-$ . The calculated value R is

$$R = 3 \sum_q e_q^2 \left\{ 1 + \frac{\alpha_s(E)}{\pi} + \frac{1.3 \alpha_s^2}{\pi^2} + \frac{m^2}{s} + \dots \right\}$$

It is expected that the perturbation expansion is good for center of mass energies larger than approximately 10 GeV. The size of the first order term proportional to  $\alpha_s$  is approximately .06 and hence one requires a 1% measurement of R to yield the desired accuracy for the value of  $\alpha_s$ . It is, however,

generally considered to be nearly impossible to experimentally obtain this level of accuracy.

A second technique for measuring  $\alpha_s$ , which we have already discussed in some detail, is to measure quantitatively the effects of gluon radiation in the hadron final state of  $e^+e^-$  interactions. As we have already noted, the effects due to the fragmentation function at PEP and PETRA energies are large and it has been demonstrated that variations in the assumptions for this fragmentation, for example, whether one uses Feynman-Field, Lund or ISAJET Monte Carlos, lead to 30% to 50% uncertainties in the value of  $\alpha_s$  determined. It is currently anticipated that the relative importance of these fragmentation effects will decrease proportional to  $1/\sqrt{s}$  and hence that at energies attainable in  $e^+e^- \rightarrow Z^0$  these uncertainties will be substantially reduced. It has, however, already been noted that contributions from heavy top quark decays may complicate the analysis somewhat.

A third technique for measuring the value of  $\alpha_s$  is to study either the moments of the structure functions or the structure functions themselves in deep inelastic scattering of electrons and neutrinos from protons or neutrons.<sup>9,10</sup> An illustration of the size of the effect anticipated as far as a change in the moments is concerned, and the minimum  $Q$  desired is

$$\frac{\partial \ln M_2(Q)}{\partial \ln Q^2} = -\frac{\gamma_2^0}{8\pi} \alpha_s (.5Q) \left\{ 1 - \frac{.3 \alpha_s}{\pi} \right\} + O\left(\frac{1}{Q^2}\right) = -.04 + O\left(\frac{1}{Q^2}\right) \quad \Lambda_{\overline{MS}} = .1$$

$+ Q^2 > 100$  at least

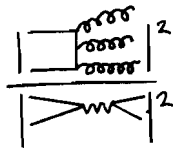
Assuming in an ep collider an accessible  $Q^2$  range of 100 to 4,000  $\text{GeV}^2$ , one anticipates a change in  $M_2$  of approximately 15%. Hence, to obtain the desired accuracy in the determination of  $\alpha_s$ , one requires a 2% accuracy in the measurement of  $M_2$ .

The structure function which is most readily obtained from deep inelastic scattering is  $F_2^{eP}$ . However, the evolution of this structure function is coupled to the evolution of the gluon structure function, which is certainly not well known. To yield an accurate test, one would like to measure the evolution of the non-singlet structure function,  $F_2^{ns} = F_2^{eP} - F_2^{en}$ . We require measurement of the structure function at all  $x$  for some  $Q_0^2$  greater than 100  $\text{GeV}^2$ . Evolution according to the renormalization group equation then predicts the value of  $F_2^{ns}$  for any other values of  $x$  and  $Q^2$ . Our requested 10% accuracy in the value of  $\alpha_s$  then demands a determination of  $F_2^{eP} - F_2^{en}$  to an accuracy of 2% to 4% as a function of  $Q^2$ .

Finally, we come to another type of test which one hopes will eventually lead to accurate determinations of  $\alpha_s$ . The branching ratio for the  $T$  decaying to a 3 gluon final state versus the decay to  $\mu^+\mu^-$  is proportional to  $\alpha_s^3$ .

$$B_{\mu\mu}^{-1}(T) \rightarrow \frac{\Gamma(T \rightarrow ggg)}{\Gamma(T \rightarrow \mu^+\mu^-)} \propto \alpha_s^3$$

↑  
terrific!



The fact that the leading term is proportional to  $\alpha_s^3$  should in principle allow a sensitive determination of  $\alpha_s$  the requisite accuracy in the value of the branching ratio is easily obtained experimentally. Unfortunately, the next higher term yields a contribution which is as large or larger than the first-order term; that is, perturbation theory fails. Whether this will remain a serious problem or not is currently unresolved.<sup>34</sup> There is hope that one may yet be able to understand the calculation sufficiently well to yield an accurate determination of  $\alpha_s$  and consequent test of QCD.

## 7. Toponium

Observation of the bound  $t\bar{t}$  state (toponium) should allow several tests of the standard model. One of these has already been noted in the discussion concerning searches for Higgs bosons. Table 12 presents the expected production rate at each of the different facilities as a function of the toponium mass. It may be seen that both  $e^+e^-$  and high luminosity pp (or pp) facilities will yield substantial number of events up to a mass of approximately 80 GeV. The expected signal to noise for production via hadron-hadron interactions is shown in Figure 17, which assumes a resolution of 1%. Similarly, Table 13 presents the expected signal to noise for  $e^+e^-$  interactions. The large rate for production of  $\Theta(t\bar{t})$  in the mass range of 80-100 GeV at  $e^+e^-$  machines results from an enhancement due to the  $Z^0$  propagator, with a consequent decrease in the signal to noise. There should be little difficulty in resolving the signal for masses up to and near the mass of the  $Z^0$ . It is generally anticipated that it will be possible to observe several, though probably not all, of the excited S states. Study of radiative transitions to P states is, however, expected to be extremely difficult.

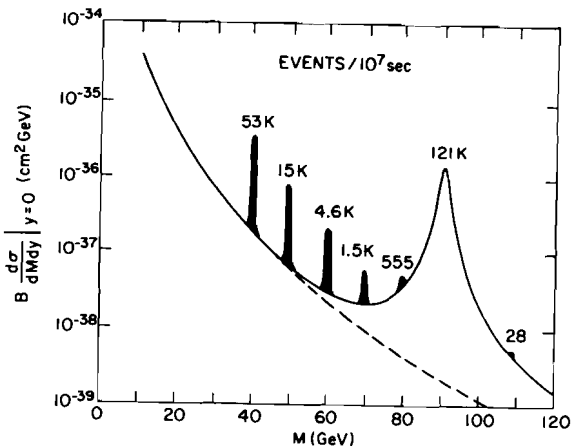


Fig. 17. Cross sections for "onium" states of various masses produced in pp collisions at  $\sqrt{s}=800$  GeV decaying into  $l^+l^-$ . Peak heights are for 1% mass resolution and event rates assume  $L=10^{33} \text{ cm}^{-2} \text{ sec}^{-1}$ .

One interesting question is at what mass does the decay of toponium begin to be dominated by the weak decay of one of the heavy quarks. Figure 18 shows the different amplitudes as a function of the toponium mass. It may be seen that, while the weak decay amplitude grows rapidly for masses in excess of approximately 60 GeV, the very strong enhancement of the normal decay mode to fermion antifermion by the virtual  $Z^0$  propagator will dominate the decays for masses between approximately 75 and 90 GeV. Above 90

**Table 12.** Toponium Production: Number of  $\mu$  Pairs/ $10^7$  sec from  $\Theta(t\bar{t}, 1S)$  at Different Machines.

	pp	$\bar{p}\bar{p}$	ep	$e^+e^-$	$e^+e^-$
W(GeV)	800	2000	140	$\leq 100$	$\leq 100$
L $\text{cm}^{-2} \text{sec}^{-1}$	$10^{33}$	$10^{30}$	$10^{32}$	$6 \times 10^{30}$	$10^{32}$
$(\delta W/W)_{\text{RMS}}$	1% (Det.)	1% (Det.)	1% (Det.)	0.5% (Machine)	$10^{-5}$ w(GeV) (Machine)
$m(\Theta)$ (GeV)	Number of $\mu^+\mu^-$ Events/ $10^7$ Sec				
40	$5 \times 10^4$	130	$10^3$	860	$1.8 \times 10^5$
60	$5 \times 10^3$	15	200	230	$3.2 \times 10^4$
80	560	3	30	70	$7.1 \times 10^3$
100	100	1	9	80	$6.6 \times 10^3$
	pp				$e^+e^-$

**Table 13.** Ground State Toponium  $\Theta$  Signals in  $e^+e^-$  as Function of Mass W Compared to "Background" of Intermediate Photon and  $Z^0$  Signals for Machine with Beam Energy Resolution  $(\delta W/W)_{\text{rms}} = 10^{-5} W$  (GeV).

W(GeV)	$R_{\text{TOTAL}}^{e^+e^- \rightarrow \text{all}}$	$\Delta R(\Theta)$	$R_{\mu\mu}^{e^+e^- \rightarrow \mu^+\mu^-}$	$\Delta R_{\mu\mu}(\Theta)$
40	6.9	33	1.01	3.3
50	7.4	21	1.03	2.1
60	9.0	14	1.08	1.3
70	14	11	1.3	0.81
80	43	11	2.2	0.53
90	830	69	28	2.4
93	5710	450	191	15
96	1020	84	35	2.8
100	248	24	9	0.76

**Notes**

- (a) Toponium parameters are determined by  $\Gamma_e(T)=5$  keV and  $\sin^2\theta_w=0.215$  in the standard model.
- (b)  $M(Z^0)=93$  GeV,  $\Gamma(Z^0)=2.62$  GeV.
- (c) Radiative corrections not included in the above entries.  $\Delta R(\Theta)$  will be reduced by a factor of 1/2, while  $Z^0$  signal at the peak will be reduced by 2/3.
- (d) Peak R values scale inversely with  $\Delta W_{\text{obs}}$ , where  $W_{\text{obs}}=2.355 \delta W_{\text{rms}}$  if  $\delta W_{\text{rms}} \gg \Gamma_{\text{total}}$  and  $W_{\text{obs}}=\Gamma_t$  in the opposite limit.

GeV, it would in any event be difficult to observe the toponium resonance. Hence, except perhaps for a narrow window in the vicinity of 70 GeV, one does not anticipate that toponium decay by the direct weak decay of the heavy quarks will be observable.

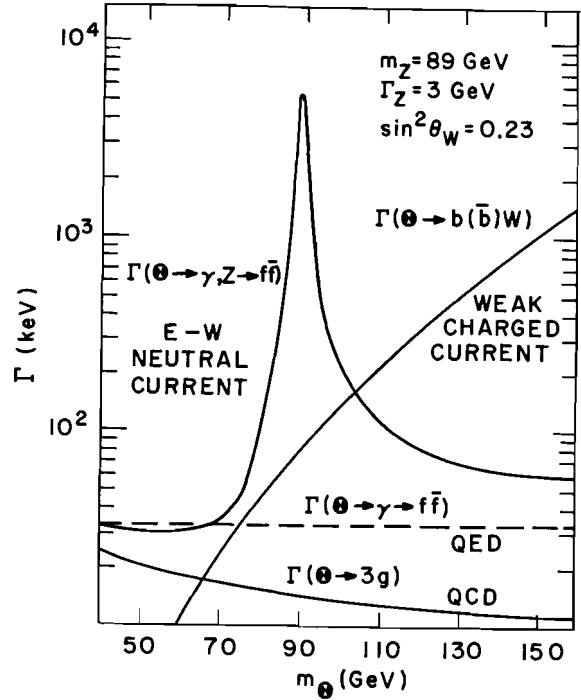


**Fig. 18.** Contributions to the width of toponium  $\Theta(t\bar{t})$  as a function of the mass of  $\Theta$ .

**8. Production of "Bare" Heavy Flavours**

It is, of course, of great interest to consider the production of heavy quarks within the context of the standard model. One thinks primarily of the t quark though one can also entertain the existence of a fourth or a fifth generation of fermions. Table 14 presents the production rates of heavy quarks for pp,  $\bar{p}\bar{p}$ , ep and  $e^+e^-$  facilities. It may again be seen that high energy or high luminosity hadron-hadron colliders, as well as the LEP II  $e^+e^-$  colliding beam facility, produce a substantial number of quarks with masses up to 100 GeV. It is in fact true that for quark masses larger than half the mass of the Z boson, the production rates are anticipated to be much larger at the hadron-hadron colliders than at the  $e^+e^-$  facility.

**Table 14.** Production of Heavy Quarks (e.g. t) per  $10^7$  seconds.

$M_Q$	$\bar{p}\bar{p}$	ISABELLE	TEVATRON
50		$1.9 \times 10^6$	$4.3 \times 10^4$
Above ↓			
LEP I 75		$10^5$	$5.7 \times 10^3$
Above ↓			
LEP II 100		$8.1 \times 10^3$	$1.2 \times 10^3$
ep	(10 x 1000 GeV)		
	Good for lower masses.		
	Little rate for $Q\bar{Q}$		
	production with $M_Q > 50$ GeV		

$e^+e^- (Z^0) \sim 10^6$  for  $M_Q < 47$  GeV

$e^+e^- (\sqrt{s}=200 \text{ GeV}) \sim 3 \times 10^3 M_Q < 100 \text{ GeV}, Q=2/3$

$\sim .75 \times 10^3 M_Q < 100 \text{ GeV}, Q=1/3$

The study of  $Z^0$  decaying into  $t\bar{t}$  (or other new quarks, should they exist) is anticipated to be especially clean. As an illustrative example, consider events selected by requiring semi-leptonic decays of either the  $t$  or  $\bar{t}$  quark in which the transverse momentum of the electron or muon relative to the jet axis is greater than 2.5 GeV. Then assuming a leptonic branching ratio of 10%, a detection efficiency for the electron or muon of 50% and that 50% of the decays satisfy the transverse momentum cut, the number of identified  $t\bar{t}$  jets per day is presented in Figure 19 as a function of the hypothesized mass of the  $t$  quark. Having identified either the  $t$  or the  $\bar{t}$  in this manner, it should then be possible to study the opposing  $\bar{t}(t)$  quark in an unbiased way with high statistics. In particular, one would expect to be able to measure the branching ratio  $t \rightarrow e\nu X$ ,  $t \rightarrow \mu\nu X$ , and to study the inclusive properties of jets from  $t$  decays. In addition, it may be possible to measure the branching ratio for  $t \rightarrow bX$  where  $b$  is the bottom quark.

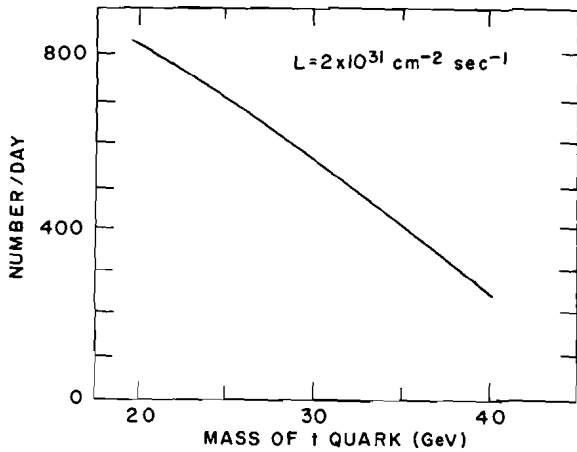


Fig. 19. Number of identified  $t\bar{t}$  jets per day vs. mass of the  $t$  quark produced from  $Z^0 \rightarrow t\bar{t}$  for  $L = 2 \times 10^{31} \text{ cm}^{-2} \text{ sec}^{-1}$ .

Identification of the decays of heavy quarks produced in hadron-hadron interactions will be more difficult but it is anticipated to be manageable, particularly if the quark is very heavy. Figure 20 shows the contribution of different processes to the dilepton mass distribution for events containing three charged leptons. Associated production of  $t$  and  $\bar{t}$  quarks yields lepton antilepton pairs with very large effective masses. While in this case, which assumes a top quark mass of 20 GeV, the contribution from  $b\bar{b}$  production is of comparable size, it is anticipated that for heavier quark masses or with additional selection criteria, the signature should be reasonably clean.

The contribution of fixed target accelerators to the study of heavy quark production is estimated to include as a minimum measurement of the lifetime of beauty particles. Table 15 presents the estimated cross section for a  $c\bar{c}$ ,  $b\bar{b}$  and  $t\bar{t}$  production both for hadron-hadron interactions and for photo production. It is particularly to be noted that for photo production the fraction of the total cross section containing  $t\bar{t}$  is not hopelessly small. Assuming  $6 \times 10^8$  interacting photons in an experiment, one anticipates the production of approximately  $7 \times 10^6$   $c\bar{c}$  pairs,  $2.5 \times 10^5$   $b\bar{b}$  pairs and on the order of  $6 \times 10^4$   $t\bar{t}$  pairs if the top quark mass is 20 GeV<sup>2</sup>.

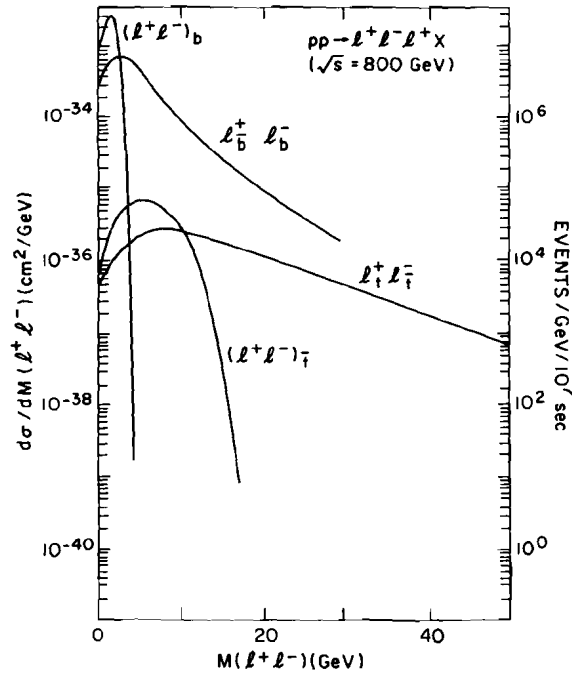


Fig. 20. Cross sections for lepton pairs from associated production of  $t\bar{t}$  and  $b\bar{b}$  quarks versus mass.  $(l^+l^-)_b$  and  $(l^+l^-)_t$  are for lepton pairs coming from the decay of the same quark.  $l_b^+l_b^-$  and  $l_t^+l_t^-$  are for lepton pairs with one lepton coming from each quark. Event scale is for  $L = 10^{33} \text{ cm}^{-2} \text{ sec}^{-1}$ .

Table 15. Production cross sections estimated for 20 TeV/c proton beam 2 TeV/c photon beam.

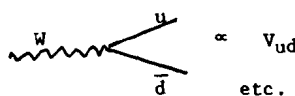
	$\sigma_{\gamma N}(\sqrt{s}=60)$	Fraction of $\sigma_{TOT}$	$\sigma_{PN}(\sqrt{s}=200)$	Fraction of $\sigma_{TOT}$
$\sigma_{TOT}$	150 $\mu$ b	1	50mb	1
$c\bar{c}+x$	2 $\mu$ b	.013	500 $\mu$ b	.01
$b\bar{b}+x$	70nb	$4 \times 10^{-4}$	3 $\mu$ b	$6 \times 10^{-5}$
$t\bar{t}+x$	$\lesssim 15$ nb	$\lesssim 10^{-4}$	2nb	$4 \times 10^{-8}$

( $M_t \approx 20 \text{ GeV}/c^2$ )

Assuming that one can reconstruct 10% of the charm decays and presuming that 50% of the  $b$  decays involve  $D$  mesons, one can in principle obtain a sample of greater than  $10^4$   $b$  decays. Determination of the top lifetime does not appear possible since it is anticipated to be less than  $10^{-16}$  seconds. Other possibilities would be the study of the  $\eta_b$  or  $\eta_t$  using photon beams, although at this time observation of the  $\eta_c$  has not been accomplished at fixed target accelerators.

#### 9. Determination of Quark Mixing Angles

It is of course known that the quark mass eigenstates are not the same as the eigenstates of the weak interaction but rather that they are related by a unitary transformation  $V$ .<sup>35</sup>

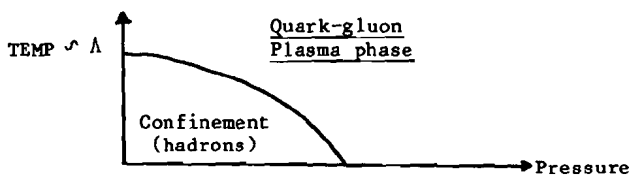
$$\begin{pmatrix} d' \\ s' \\ b' \end{pmatrix} = V \begin{pmatrix} d \\ s \\ b \end{pmatrix} = \begin{pmatrix} V_{ud} & V_{us} & V_{ub} \\ V_{cd} & V_{cs} & V_{cb} \\ V_{td} & V_{ts} & V_{tb} \end{pmatrix} \begin{pmatrix} d \\ s \\ b \end{pmatrix}$$


etc.

where  $q(q')$  denote mass (weak) eigenstates and the quark mixing matrix  $V$  is a function of four real parameters in the case of  $n=3$  generations. Of these four parameters, 3 are CP conserving rotation angles and the fourth is a CP violating phase. Specifically  $V = V(\theta_1, \theta_2, \theta_3, \delta)$ . The explicit forms for the two most accurately determined matrix elements are  $V_{ud} = \cos\theta_1$ , and  $V_{us} = \sin\theta_1 \cos\theta_3$ . A review was given in this study by R. Shrock.<sup>36</sup> Here we simply summarize some of the highlights. Measurement of muon decay and nuclear  $\beta$  decay imply that  $\cos\theta_1 = 0.9737 \pm 0.0025$ . A generalized Cabibbo fit implies that  $V_{us} = 0.219 \pm 0.002$  (statistical)  $\pm .01$  (estimated theoretical uncertainty). To get bounds on other parts of  $V$ , one may analyze processes where heavy quarks couple to light ones, such as  $K^0 \bar{K}^0$  mixing and  $K_L \rightarrow \mu^+ \mu^-$ . Information on these two processes yielded correlated bounds on  $\sin\theta_2$  and  $\sin\theta_3$ . Charm decays will give information on  $V_{cd}$  and  $V_{cs}$ , while B decays similarly will yield information on  $V_{ub}$  and  $V_{cb}$ . One already has the CESR result that the magnitude of  $V_{cb}$  is substantially greater than the magnitude of  $V_{ub}$ . This follows both from the number of kaons observed and also from measurements of the lepton momentum spectra from semi-leptonic decays. Further study of charm decays in the MARK III experiment at SPEAR and of B decays in the detectors at CESR should improve our knowledge of  $V$ .

#### 10. Relativistic Heavy Ion Collisions

Finally we note that some consideration has been given to the importance of relativistic heavy ion collisions in testing the standard model. The objective is to create a quark-gluon plasma by obtaining sufficiently high temperatures and pressure. It is conjectured, or at least hoped, that sufficient energy can be deposited in the nuclear fragmentation regions to cause the phase transition.



Although it does not appear to be a reliable guide for estimation of the phase transition probability in relativistic heavy ion collisions, the idea is nonetheless considered to be very intriguing and it is noted that QCD could lead to unexpected effects. It is also pointed out that it may be possible to do heavy ion fixed target experiments, for example, at the CERN-SPS and/or perhaps at the AGS, in a sufficiently interesting kinematical regime before dedicating a new facility to these studies.

#### References

1. ISABELLE - Proceedings of the 1981 Summer Workshop, BNL-51443 (1981).

2. Proceedings of Topical Workshop on Production of New Particles in Super High Energy Collisions, Madison, Wisconsin (1979).
3. Proceedings of the LEP Summer Study, Les Houches and CERN, 10-22 September, 1978, CERN 79-01 (1979).
4. Proceedings of the Cornell  $Z^0$  Theory Workshop, February 6-8, 1981, CLNS 81-485 (1981).
5. Proceedings of the SLC Workshop on Experimental Use of the SLAC Linear Collider, SLAC-247 (1982).
6. W. Marciano and Z. Parsa, Predicted Properties of the  $W^\pm$  and  $Z^0$ , these proceedings.
7. M.R. Adams et al., Large Angle Particle DO Group (LAPDOG) Proposal P714 for Tevatron-I, 1982.
8. G. Bunce et al.,  $W, Z^0$  Production at a PP Collider, these proceedings.
9. Proceedings of the Study of an EP Facility for Europe DESY Hamburg, April 2-3, 1979, DESY 79/48 (1979).
10. Report of the Electron Proton Working Group of ECFA, Study on the Proton-Electron Storage Ring Project-HERA, ECFA 80/41 (1980).
11. Canadian High Energy Electron Ring (CHEER), Sept. 1980.
12. T.A. O'Halloran, Jr., Lepton-Hadron Colliders, these proceedings.
13. B. Gittelmann, et al., The  $Z^0$  Factory, these proceedings.
14. P. Grannis, private communication.
15. G. Barbiellini, B. Richter and J.L. Siegrist, Phys. Lett. 106B, 414 (1981).
16. J. Kim, et al., Rev. Mod. Phys. 53, 211 (1980).
17. K. Abe, F. Taylor and D.H. White, Measurement of  $V_e$  and  $V_e$  Elastic Scattering as a Test of the Standard Model, these proceedings.
18. R. W. Brown and K.O. Mikaelian, Phys. Rev. D19, 922 (1979).
19. R.W. Brown, D. Sahdev and K.O. Mikaelian, Phys. Rev. D20, 1164 (1979).
20. M.A. Samuel, private communication.
21. For a review see A. Ali, reference 1, p. 194.
22. J.D. Bjorken, 1976 SLAC Summer Institute Proceedings.
23. R. Chan, M. Chanowitz and N. Fleisham, Phys. Lett. 82B, 113 (1979).
24. M. Goldberg, private communication.
25. H. Gordon, et al., Heavy Higgs Production and Detection, these proceedings, and M. Peskin, private communication.
26. H. Georgi, et al., Phys. Rev. Lett. 40, 692 (1978).



27. CELLO Collaboration, submitted to the 1981 International Symposium on Lepton and Photon Interactions at High Energies Bonn, (1981).
28. G. Fox, private communication.
29. T. Akesson, et al., Direct Evidence for the Emergence of Jets in Events Triggered on Large Transverse Energy at  $\sqrt{s}=63$  GeV, (to be published in Phys. Lett.) CERN-EP/82-138. M. Banner, et al., Observation of Very Large Transverse Momentum Jets at the CERN pp Collider (to be published in Phys. Lett.) CERN-EP/82-141.
30. F.E. Paige and S. Protopopescu, ISAJET: A Monte Carlo Generator for pp and pp Interaction. Version 3, these proceedings.
31. R. Baier, et al., Z. Phys. C2, 265 (1979).
32. M. Tanaka, private communication.
33. M. Tannenbaum, Standard Model Group, QCD Subgroup-Dynamics. Isolating and Testing the Elementary QCD Subprocesses, these proceedings.
34. P. Lepage, these proceedings.
35. See for example, Ling-Lie Chau, Quark Mixing in Weak Interactions, to be published in Physics Reports, BNL-31859 (1982).
36. R. Shrock, these proceedings.